COMMUNICATION

A Supramolecular Sensor Array for Selective Immunoglobulin Deficiency Analysis

Received 00th January 20xx,
Accepted 00th January 20xx

DOI: 10.1039/x0xx00000x

Yang Liu,[a] Adam D. Gill,[c] Yaokai Duan,[b] Lizeth Perez,[b] Richard J. Hooley*[b,c] and Wenwan Zhong*[a,b]

A host-guest based fluorescence sensor array can sense small differences in protein structure. The combination of three cavitand hosts and two fluorophores to form a 4-component array is sufficient to fully discriminate five structurally similar Ig protein isotypes. The array can be applied to recognize Ig deficiencies in serum, when combined with a Protein L-based extraction process, allowing analysis of immunodeficiency in a simpler, lower cost manner than tests that require multiple specific antibodies.

Detection of protein biomarkers is commonly performed with highly selective antibody-based probes which have diverse applications in clinical practices and therapeutic development. [1] However, each target requires its own selective probe, which is time consuming and costly, and differentiation between protein homologs remains challenging.[2] An alternative and simpler strategy is to use "chemical nose" sensing, which employs arrayed hosts as the recognition elements.[3] This relies on different interactions between the targets and multiple molecular recognition elements to generate signaling patterns that can be easily distinguished by statistical tools. The benefits include simplicity and low cost, as well as the *pan*-selectivity of synthetic receptors that can be adapted to different targets with strategic tuning.[3] Diverse recognition elements such as synthetic receptors, [3c,3d] fluorescent proteins[4] and nanoparticles[5] have been explored, and have allowed detection of a wide range of analytes, including volatile organic compounds, [6] environmental contaminants, [7] peptide modifications, [8] and even cell phenotypes. [9]

Still, a major challenge in chemical nose array sensing is to distinguish analytes with complex secondary and tertiary structures, like protein isotypes. Arrayed sensors that have been previously applied to differentiate proteins use large recognition units that can exploit multivalency in recognition. [10] Even then, the protein targets are restricted to those that have large differences in molecular weight (M_w), isoelectric point (pI), and surface features. For example, arrays using fluorescent or colorimetric nanoparticles (NPs) mainly rely on the charged surface ligands on the NPs forming electrostatic, H-bonding, π-π stacking, or hydrophobic interactions with the protein surface. [11] Peptide chains have also been employed to interact with the core analyte-binding unit, allowing differential binding. [12] However, lack of specificity in target recognition limits the applicability of these arrays towards differentiating protein isotypes. There are some elegant examples that integrate specific protein binders with the spectrally overlapping solvatochromic dyes and FRET pairs to discriminate protein isotypes, but these require multistep synthesis of suitable fluorophore-receptor conjugates. [13]

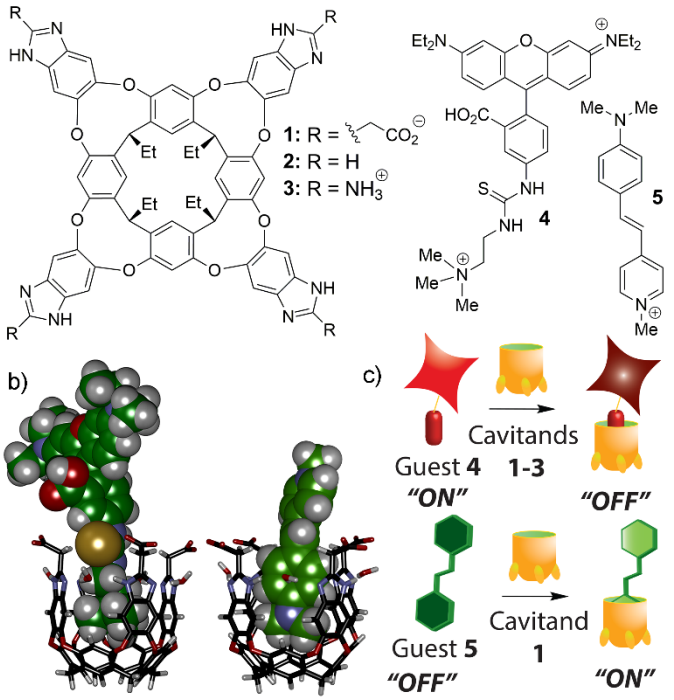

Fig. 1. a) Structure of hosts **1**-**3**, guests **4** and **5**; b) minimized models of the **1**•**4** and **1**•**5** host:guest complexes (SPARTAN); c) Illustration of the turn-on and turn-off fluorescence detection processes.

[a] University of California - Riverside, Environmental Toxicology Program, Riverside, CA, 92521, U.S.A. E-mail: wenwan.zhong@ucr.edu;
[b] University of California - Riverside, Department of Chemistry, Riverside, CA, 92521, U.S.A. E-mail: richard.hooley@ucr.edu.
[c] University of California - Riverside, Department of Biochemistry and Molecular Biology, Riverside, CA, 92521, U.S.A.

Electronic Supplementary Information (ESI) available: experimental procedures and fluorescence data. See DOI: 10.1039/x0xx00000x

Here, we show a cavitand-based sensor that is capable of differential sensing of protein isotypes and apply it to analyze immunoglobulin Ig deficiency. Ig proteins are homologous Y-shaped members of the same family that are distinct in their C regions.[14] Five members in the Ig family, IgA, IgG, IgM, IgE and IgD, are present in serum and can provide key information on patient's immune status.[15] The reference intervals of the three most abundant Ig proteins for healthy adults are: IgA 70–400 μg/ml, IgG 700–1600 μg/ml and IgM 40–230 μg/ml;[15] but deficiencies in even one of the isotypes are linked to increased risk for allergies, autoimmune diseases, and tumor development. Levels of all Ig protein subtypes are determined in clinical practice by radial immunodiffusion assays (RID), [16] ELISAs[17] and nephelometric immunoassays. [18] These assays require multiple antibodies, which can suffer from crosstalk due to their high sequence and structural similarity of these proteins.[14] Moreover, it is often necessary to analyze the differential expression profiles of all five Ig proteins simultaneously. An assay that can rapidly recognize the deficiency in one type of Ig protein by screening several Ig members in a cost-effective manner without using antibodies remains attractive.

Recently, we have developed deep cavitand-based sensor arrays that can be used to sense post-translational modifications (PTM) in peptide strands, [19] showing selective discrimination between different types of modifications, modifications at different residues, [20] and even between identical modifications at different positions on the peptide backbone. [21]

We created the sensor array using three cavitands (**1**, **2** and **3**) and two fluorescent guest molecules (**4** and **5**) (Fig. 1). Guest **4**, a Rhodamine B based fluorophore, binds to all three cavitands at pH 3.0 - 9.0, and the binding strongly quenches its fluorescence. In contrast, guest **5** exhibits a large increase in fluorescence upon binding to cavitand **1**, something not observed with hosts **2** or **3**. These cavitand-dye pairs have been proved to be highly sensitive to the changes in the microenvironment around modified amino acids in peptide strands. [21] As Ig proteins are unstable at low pH, we only applied two sets of pH conditions to the array. The full 8-factor array consisted of the host-guest complexes **1·4**, **2·4** or **3·4** at pH 7.4 or 9.0 (10 mM PBS or carbonate buffer, respectively) with [**4**] = 3 μM and that of cavitand **1**, **2** and **3** being 4, 5, and 5 μM, respectively, and **1·5** at pH 7.4 with [**5**] = 1.5 or 40 μM.

This sensing array was initially applied to samples of the three most structurally different isotypes, IgG, IgM, and IgA (which have Mw = 150, 970 and 320 kDa, respectively). The fluorescence profile of the array resulting from mixing each sensor with 150 μM of each the three Ig proteins is shown in Fig. 2a. We can see that the fluorescence of **1·5** and **1·4** (pH 7.4) increased the most, by 2.5-3.5 and 1.5-2.5 fold, respectively. The largest protein, IgM, induced the largest fluorescence change, and the response pattern of each isotype was quite distinct from that of others. Principal component analysis (PCA) (Fig. S-1) and Jackknife analysis (Table S-3) on the fluorescence patterns showed good differentiation among IgA, IgG, IgM and the no-protein control. Studying the loading scores (Table S-2) from this initial PCA determined that the sensors **1·4**, **2·4**, **3·4** and **1·5** (at a ratio of 1:25) at pH 7.4 made the most important contributions to the grouping effect. As such, we applied this minimal array to the differentiation of all 5 Ig proteins, including IgD, and IgE, which are highly structurally similar to IgG and present a far more stringent sensing challenge. Five repeated measurements on IgG, IgM, IgA, IgD, and IgE were conducted with this array, and the emission profile and scores plots from PCA are shown in Figs. 2b,c. The PCA scores plot exhibited excellent discrimination between the individual Ig isotypes, with the repeated analysis of each Ig protein tightly enclosed in the 95% confidence ellipse. Despite IgM, IgD and IgE having highly comparable pI values, hydrophobicity, and tertiary structures, with many regions having conserved amino acid sequences (Table S1), good separation can be obtained with a minimal array, showing the effectiveness of this simple cavitand:guest recognition system. The sensing is both selective and sensitive: the response was quantified and sensor **1•4** gave the lowest detection limit at 0.77 μg/mL, equivalent to about 1,000 fold dilution of the Ig protein levels in the serum of a healthy individual (Fig. S-2).

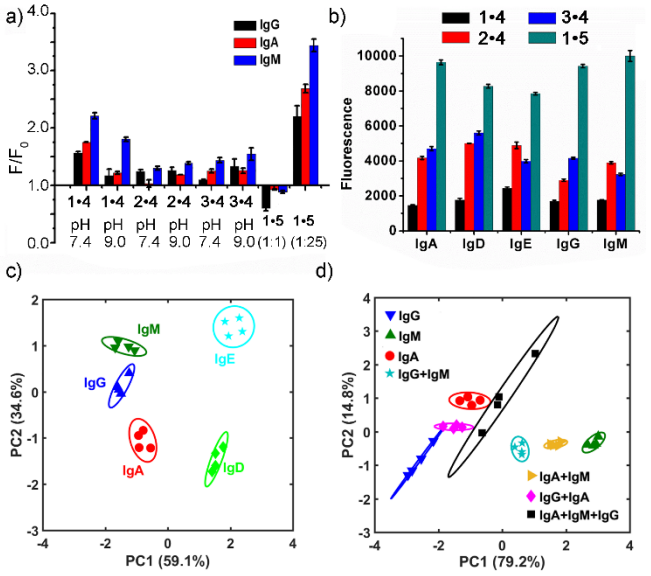

Fig. 2. a) Cavitand:guest response to IgG, IgA and IgM; b) fluorescence data of all five Ig proteins with the minimal **1·4**, **2·4**, **3·4**, **1·5** sensor array; c) PCA plot of five immunoglobulin proteins; d) protein mixtures test with IgA, IgG and IgM. 95% error ellipse was shown surrounding the clusters. [Ig protein] = 150 μg/mL. F_0: sensor fluorescence without protein. Error ellipses were obtained at 95% confidence interval.

We further challenged our array to detect different isotypes in mixtures of proteins. Seven protein mixtures were created, keeping the [total protein] = 150 μg/mL and varying proportions of IgG, IgM, and IgA, and were exposed to the minimal array. The scores plot from PCA on the fluorescence profiles of these protein samples shows good separation in all cases (Fig. 2d, for fluorescence profiles, see Fig. S-3). Interestingly, the two-protein samples (IgA + IgG, IgA + IgM, IgG + IgM) are positioned in-between the single-protein samples containing the two proteins involved. Similarly, the three-protein mixture (IgA + IgG + IgM) resides close to the center of the triangle established by

the three single-protein samples containing only IgG, IgA, or IgM. This shows that the array can differentiate isotypes in Ig protein mixtures, which introduces the possibility of detecting Ig protein depletion in clinical samples collected from patients with immunodeficiencies. We thus tested whether our array could tell apart samples mimicking decreasing concentration in one of the Ig proteins, like IgG. We prepared the mixture of IgA and IgM at an equal mass concentration of 50 μg/mL in 1xPBS, and added varied concentrations of IgG ranging from 0 to 400 μg/mL. The mixture containing no IgG (IgA: IgM: IgG =1:1:0) represents the state of complete IgG depletion, and that with IgA: IgM: IgG being 1:1:8 mimics the healthy range. All samples were significantly distinguishable by the 4-factor array at a confidence level of 95% (Fig. S-4). Most excitingly, the samples mimicking the situations of IgA, IgG, or IgM deficiency can be clearly differentiated from the mixture containing all three Ig proteins at the ratio of IgA: IgM: IgG =1:1:8, i.e. the mimic of "normal" condition, with all four situations well separated from each other (Fig. S-5).

While the array is obviously successful in detecting different protein isotypes, it is challenging to determine why this is so. The initial screening shows that the Ig proteins reverse the quenching effect of the cavitands on guest **4**, and further increase the fluorescence of guest **5**. These responses are not simply due to interaction of the host with the protein, followed by fluorophore displacement: increasing emission of **4** is likely due to displacement and reduced quenching, but guest **5** is turned on upon binding to cavitand **1**, so displacement would reduce the fluorescence. This fluorogenic molecule is sensitive to hydrophobic environments, which suggests an interaction between the cavitand:guest complexes and the Ig proteins.

To gain more information on the mechanism of sensing and the host:Ig binding process, we studied the intrinsic fluorescence originating from tryptophan residues in IgM, which can be quenched if within Förster distance of bound host.[20] The emission spectra of IgA, IgM and IgE upon binding to cavitand **1** at increasing concentration are shown in Fig. S-6. In each case, peak fluorescence at λ = 320-340 nm gradually decreased with increasing [**1**], and the λ_{max} exhibited a significant blue-shift. The blue shift in tryptophan's λ_{max} is evidence for the averaged microenvironment around tryptophan changing from being hydrophilic to hydrophobic, and the fluorescence intensity decrease hints potential quenching of tryptophan fluorescence upon cavitand binding. We also employed limited proteolysis[22] on IgM before and after incubation with cavitand **1** to investigate which amino acid regions on IgM were bound by the host. The peptides cleaved by a 10-min trypsin digestion step (Fig. S-7) were identified by LC-MS/MS and their relative contents were evaluated semi-quantitatively by spectra counting. Incubation with cavitand **1** prevented digestions of the amino acid residues from # 75-125, as well as those between #350 and #400, while enhanced cleavage was observed for those located between #150 and #200 (Fig. S-8). The affected regions are the Fc regions of IgM, which have higher percentage of hydrophobic residues than average of the whole sequence. These results suggest that the lipophilic cavitands likely interact with the Ig protein regions with relatively higher hydrophobicity, causing changes in the fluorescence of bound guests **4** and **5**. We also noticed two tryptophan residues were adjacent to (#148) or included within (#365) these affected regions, partially supporting the tryptophan quenching behaviour observed in Fig. S-6.

While the cavitand array was highly effective in discriminating between Ig isotypes in controlled systems, even being able to detect variations in individual Ig protein concentrations in protein mixtures, the real goal is to analyze Ig proteins in serum. The challenge is that serum contains a variety of other constituents that could interact with the cavitands and prevent detection of the target Ig proteins. To overcome this difficulty, we used magnetic beads conjugated with Protein L to isolate the Ig proteins from the complex serum matrix prior to detection by the cavitand array. Protein L has high affinity to all five Ig proteins (IgG, IgM, IgA, IgE and IgD) through binding to their kappa light chains. Fig. 3 shows the schematic: protein L beads bind to the Ig proteins in serum, then after removal of the beads and elution of the bound Ig proteins, the selective recognition of each individual Ig isoform can be assayed by the cavitand array.

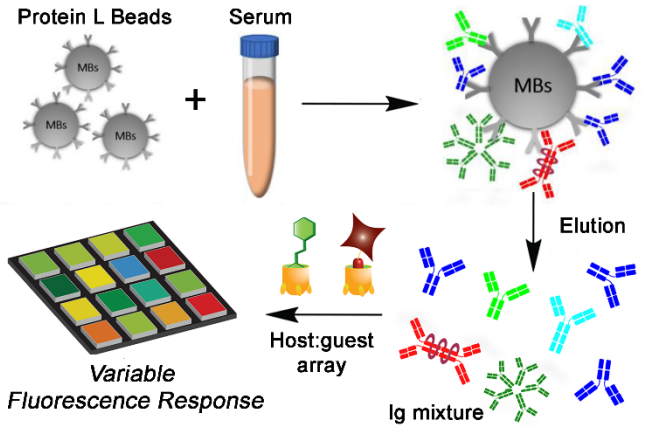

Fig. 3. Scheme of the serum protein immunoglobulin detection. Protein L magnetic beads (MBs) were first mixed with serum, and extracted Immunoglobulins were eluted and measured using the cavitand-guest sensor array.

The commercially available Protein L beads exhibited reasonable recovery for the Ig proteins in serum: with only 0.125 mL of beads, the average extraction efficiency of IgA, IgG, and IgM was about 42%, 60%, and 51%, respectively, in the protein mass range of 3 – 60 μg (Table S-4). Such a protein mass range was selected according to the Ig protein levels found in healthy people with the consideration that only tens of μL of the serum sample would be used for detection of the Ig proteins. On average, 81% of the extracted Ig proteins could be eluted from the beads by the acidic glycine buffer (pH 2) (Table S-5), with the extracted proteins quantified by ELISA.

The Ig protein mixtures representing "normal" concentrations in serum (IgA = 200 μg/mL, IgM = 200 μg/mL and IgG = 1600 μg/mL), or that of IgA, IgG, or IgM deficiency were spiked to a serum sample initially depleted of all Ig proteins. Then the proteins were extracted by the Protein L beads, eluted by glycine buffer, neutralized by sodium hydroxide, and subjected to analysis by our cavitand array. Varied fluorescence

patterns were generated for each sample (Fig. 4a), and PCA resulted in a similar clustering pattern (Fig. 4b) as that obtained from analyzing the same protein mixtures prepared in 1xPBS (Fig. S-5), demonstrating the effectiveness of the Protein L beads in removing all the background molecules while keeping the Ig protein profile intact. For comparison, the Ig protein samples were also analyzed by ELISA. Using three discrete antibodies and three calibration curves (Fig. S-9) allowed the concentration of each Ig protein to be determined (Fig. 4c). Subjecting the chemiluminescence profiles obtained by ELISA to PCA, the four samples were also well differentiated, with a similar grouping pattern and comparable separation distances between different groups (Fig. 4d) to that obtained with our array (Fig. 4b). This result confirms the accuracy of the cavitand-based sensor, and also illustrates its benefits: the arrayed sensor can perform as well as ELISA assays, and does so with simple fluorescence responses instead of the complexity of the ELISA process that requires multiple specific antibodies.

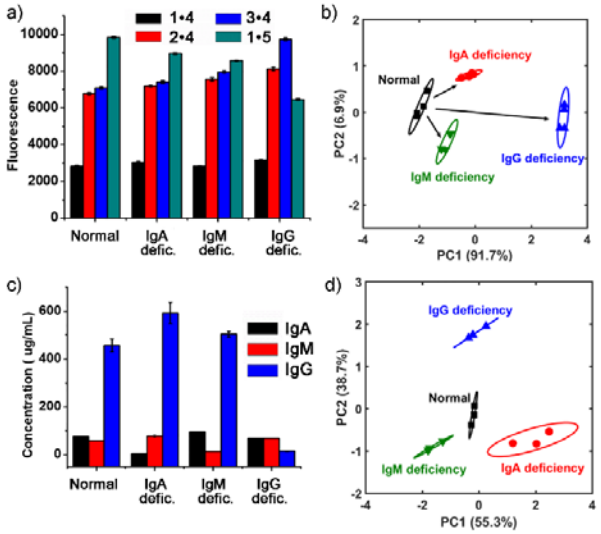

Fig. 4. Spiked serum sample detection using sensor array. Immunoglobulin depleted serum was spiked with different mass ratios of IgA, IgM and IgG. **Normal:** IgA: IgM: IgG = 1:1:8; **IgA deficiency:** IgA: IgM: IgG = 0:1:8; **IgM deficiency:** IgA: IgM: IgG = 1:0:8; **IgG deficiency:** IgA: IgM: IgG = 1:1:0. a) fluorescence response of four serum samples to the 1·4, 2·4, 3·4, 1·5 array; b) PCA scores plot from the fluorescence response; c) ELISA quantification of each immunoglobulin concentration d) PCA scores plot from ELISA results. The error ellipses were obtained at 95% confidence interval.

In conclusion, we have demonstrated the use of an arrayed host:guest indicator system to differentially sense Ig protein isoforms that have high structural similarities. The host molecules are sensitive to hydrophobic regions in proteins, and when mixed with different fluorophores, can discriminate small differences in protein structure. The array is capable of discriminating proteins in controlled media, and can be applied to analyzing Ig deficiencies in serum, when combined with a Protein L-based extraction process. This sensor can assess immunodeficiency in a simpler, and lower cost manner than antibody-based tests.

The authors would like to thank the National Science Foundation (CHE-1707347) for support.

Conflicts of interest

There are no conflicts to declare.

Notes and references

1 N. Rifai, M. A. Gillette, S. A. Carr, *Nat. Biotechnol.* 2006, **24**, 971.
2 a) K. Yamamoto, M. Shiroo, S. Migita, *Science* 1986, **232**, 227; b) L. M. Smith, N. L. Kelleher, *Nat. Methods* 2013, **10**, 186.
3 a) J. R. Askim, M. Mahmoudi, K. S. Suslick, *Chem. Soc. Rev.* 2013, **42**, 8649; b) Y. Geng, W. J. Peveler, V. M. Rotello, *Angew. Chem.* 2019, **131**, 5244; *Angew. Chem., Int. Ed.* 2019, **58**, 5190; c) A. P. Umali, E. V. Anslyn, *Curr. Opin. Chem. Biol.* 2010, **14**, 685; d) Z. Li, J. R. Askim, K. S. Suslick, *Chem. Rev.* 2019, **119**, 231.
4 M. De, S. Rana, H. Akpinar, O. R. Miranda, R. R. Arvizo, U. H. F. Bunz, V. M. Rotello, *Nat. Chem.* 2009, **1**, 461.
5 U. H. F. Bunz, V. M. Rotello, *Angew. Chem.* 2010, **122**, 3338; *Angew. Chem., Int. Ed.* 2010, **49**, 3268.
6 a) Z. Zhang, D. S. Kim, C.-Y. Lin, H. Zhang, A. D. Lammer, V. M. Lynch, I. Popov, O. S. Miljanić, E. V. Anslyn, J. L. Sessler, *J. Am. Chem. Soc.* 2015, **137**, 7769; b) S. H. Lim, L. Feng, J. W. Kemling, C. J. Musto, K. S. Suslick, *Nat. Chem.* 2009, **1**, 562.
7 Y. Liu, T. Minami, R. Nishiyabu, Z. Wang, P. Anzenbacher, *J. Am. Chem. Soc.* 2013, **135**, 7705.
8 a) Y. Liu, L. Perez, A. D. Gill, M. Mettry, L. Li, Y. Wang, R. J. Hooley, W. Zhong, *J. Am. Chem. Soc.* 2017, **139**, 10964; b) B. C. Peacor, C. M. Ramsay, M. L. Waters, *Chem. Sci.* 2017, **8**, 1422; c) K.D. Daze, F. Hof, *Acc. Chem. Res.* 2013, **46**, 937; d) K.D. Daze, T. Pinter, C.S. Beshara, A. Ibraheem, S.A. Minaker, M.C. Ma, R.J. Courtemanche, R.E. Campbell, F. Hof, *Chem. Sci.* 2012, **3**, 2695.
9 A. Bajaj, O. R. Miranda, I. B. Kim, R. L. Phillips, D. J. Jerry, U. H. F. Bunz, V. M. Rotello, *Proc. Natl. Acad. Sci. USA* 2009, **106**, 10912
10 A. T. Wright, M. J. Griffin, Z. Zhong, S. C. McCleskey, E. V. Anslyn, J. T. McDevitt, *Angew. Chem.* 2005, **117**, 6533; *Angew. Chem., Int. Ed.* 2005, **44**, 6375.
11 H. Kong, Y. Lu, H. Wang, F. Wen, S. Zhang, X. Zhang, *Anal. Chem.* 2012, **84**, 4258.
12 a) D. Zamora-Olivares, T. S. Kaoud, K. N. Dalby, E. V. Anslyn, *J. Am. Chem. Soc.* 2013, **135**, 14814; b) W. R. Algar, M. G. Ancona, A. P. Malanoski, K. Susumu, I. L. Medintz, *ACS Nano* 2012, **6**, 11044.
13 a) Z. Pode, R. Peri-Naor, J. M. Georgeson, T. Ilani, V. Kiss, T. Unger, B. Markus, H. M. Barr, L. Motiei, D. Margulies, *Nat. Nanotech.* 2017, **12**, 1161; b) J. Hatai, L. Motiei, D. Margulies, *J. Am. Chem. Soc.* 2017, **139**, 2136.
14 a) H. W. Schroeder Jr, L. Cavacini, *J. Allergy Clin. Immunol.* 2010, **125**, S41; b) K.-i. Kuma, N. Iwabe, T. Miyata, *Curr. Opin. Struct. Biol.* 1991, **1**, 384.
15 A. Gonzalez-Quintela, R. Alende, F. Gude, J. Campos, J. Rey, L. M. Meijide, C. Fernandez-Merino, C. Vidal, *Clin. Exp. Immunol.* 2008, **151**, 42.
16 M. D. Curry, A. Gustafson, P. Alaupovic, W. J. McConathy, *Clin. Chem.* 1978, **24**, 280.
17 C. Hennig, L. Rink, U. Fagin, W. J. Jabs, H. Kirchner, *J. Immunol. Methods* 2000, **235**, 71.
18 J. R. Delanghe, J. P. Chapelle, S. C. Vanderschueren, *Clin. Chem.* 1990, **36**, 1675.
19 Y. Liu, L. Perez, M. Mettry, C. J. Easley, R. J. Hooley, W. Zhong, *J. Am. Chem. Soc.* 2016, **138**, 10746.
20 Y. Liu, L. Perez, M. Mettry, A. D. Gill, S. R. Byers, C. J. Easley, C. J. Bardeen, W. Zhong, R. J. Hooley, *Chem. Sci.* 2017, **8**, 3960.
21 Y. Liu, J. Lee, L. Perez, A. D. Gill, R. J. Hooley, W. Zhong, *J. Am. Chem. Soc.* 2018, **140**, 13869.
22 Y. Feng, G. De Franceschi, A. Kahraman, M. Soste, A. Melnik, P. J. Boersema, P. P. de Laureto, Y. Nikolaev, A. P. Oliveira, P. Picotti, *Nat. Biotechnol.* 2014, **32**, 1036.

A Supramolecular Sensor Array for Selective Immunoglobulin Deficiency Analysis

Yang Liu,[a] Adam D. Gill,[c] Yaokai Duan,[b] Lizeth Perez,[b] Richard J. Hooley[b],[c] and Wenwan Zhong[a],[b]**

[a] Environmental Toxicology Program; [b] Department of Chemistry; [c] Department of Biochemistry and Molecular Biology; University of California-Riverside, Riverside, CA 92521, U.S.A.

richard.hooley@ucr.edu; wenwan.zhong@ucr.edu

Electronic Supplementary Information

Table of Contents

Experimental Section

General Information. Cavitands **1**,[1] **2**,[2] **3**[3] and guest **4**[3] were synthesized according to literature procedures. DSMI **5** (trans-4-[4-(Dimethylamino)styryl]-1-methylpyridinium iodide) was purchased from Sigma-Aldrich (St. Louis, MO) and used without further purification. Immunoglobulin isotypes including IgA, IgG and IgM were purchased from sigma-Aldrich (St. Louis, MO); IgD and IgE were purchased from Abcam (San Francisco, CA). Rabbit anti-human Immunoglobulin (IgA, IgG and IgM) with HRP was also purchased from Abcam. Immunoglobulin depleted human serum was purchased from Celprogen (Torrance, CA). Pierce™ Protein L Magnetic Beads were purchased from Thermo Fisher Scientific (Waltham, MA). All buffers were prepared with ultrapure water.

Principal Component Analysis (PCA) was accomplished with RStudio (Version 1.0.136), an integrated development environment (IDE) for R (version 3.3.2). Jackknife test was also conducted with RStudio. Confidence ellipses were drawn with the data obtained from PCA using Matlab (version R2016b) and a self-developed script.

Experimental Procedures.

Gel electrophoresis. The PAGE gel prepared includes two parts: the top staking gel (4%) and bottom separation gel (13%). 10 μL of immunoglobulin and cavitand mixture was first mixed with 10 μL of 2X Laemmli Sample Buffer (BIO-RAD, Hercules, CA). 12 μL of the above mixture was applied to each lane. The gel was run at room temperature for 30 minutes with 200 voltages. After running, the gel was stained with QC Colloidal Coomassie Stain (BIO-RAD, Hercules, CA), following recommended procedures.

Measurement of Fluorescence Displacement. In a typical displacement assay, 2 μL of the fluorescent guest (**4** or **5**) ([**4**] = 30 μM, [**5**] = 400 μM), 2 μL of the cavitand **1**, **2** or **3** ([**1**] = 40 μM, [**2**] = 50 μM, [**3**] = 50 μM), 4 μL Immunoglobulin protein, and 12 μL of the 1×PBS (10 mM phosphate at pH 7.4 with 150 mM NaCl) were mixed in the 384-well plate, and incubated with mild shaking for 10 minutes. Followed, fluorescence was recorded in a Perkin Elmer Wallac 1420 Victor 2 Microplate Reader (PerkinElmer, Inc., Waltham, MA) with the Ex/Em wavelengths at 530/605 nm for guest **4** or 485/605 for guest **5**.

Tryptophan quenching assay for binding exploration. Tryptophan quenching assay was carried out on a Horiba QM-400 Fluorometer with excitation at 280 nm. With 400 μg/mL Ig

protein in PBS (10 mM, PH 7.4), cavitand **1** concentration was increased from 2.5 μM to 167.5 μM. Emission spectrum was taken after each addition.

Limited proteolysis for binding exploration. Limited proteolysis was used here to study the binding between immunoglobulin and cavitand. This method carries out very brief digestion on the protein to identify which peptides have better accessibility to the protease. Since ligand interaction could either block the peptides at the interface, thus reducing their digestion, or could change protein conformation, releasing more cleavage sites, this method can reveal the peptides locating at the binding interface. Initial inspection of the proteolysis rates of the three Ig proteins, in which the protein was digested by trypsin at various duration (10, 60, 120 min.) and the resulting protein samples were subject to SDS-PAGE, showed that, the presence of cavitand could enhance the digestion efficiency of IgG and IgM, with 20% (for IgG) to 30% (for IgM) being digested even within 10-min proteolysis treatment (see Figure S-3). No obvious change was observed for IgA. Thus, IgM was chosen for limited proteolysis to explore the potential interaction interface. In a typical process, immunoglobulin protein (0.5 mg/mL) was first treated with TCEP and IAA as described above. Then, cavitand (0.5 mg/mL) was added into the treated immunoglobulin protein solution to a final mass ratio of 1:1 and incubated for 1 hour at room temperature. Trypsin was added to above solution with a final trypsin to protein ratio of 1:50. After 10 minutes digestion at 37℃, the reaction was stopped by adding 8 M urea. A final concentration of 5 mM DTT was added and incubated at 60℃ for 30 minutes. After that, IAA was added with a final concentration of 10 mM at incubated for another 20 minutes. The resulted solution was separated with 30 KD Amicon Ultra Centrifugal filter. The passthrough were collected and further digested with trypsin again at 37 ℃ overnight. The sample was cleaned by ziptip before injection into the LC MS/MS (Thermo Scientific LTQ). Data was analyzed by comparing the identified peptide with the protein amino acid sequence.

Protein L bead extraction. The extraction of immunoglobulin from sample solution was carried out following recommended product protocols with small modification. In a typical run, 25 μL beads and 75 μL of TBS buffer (Tris-Buffer saline containing 0.05% Tween-20) were added into 1.5 mL centrifugal tube and vortexed gently to mix. After magnetic pull down, the supernatant was discarded, and another 1 mL TBS buffer was added to do a second wash. After washing, samples with immunoglobulin proteins was added into the pre-cleaned beads and incubated for 1 hour with gentle mixing. The beads were then collected and washed twice with 1 mL TBS buffer.

Elution of bounded immunoglobulin was done with glycine buffer (100 mM, pH 2) and pHs were further neutralized with Tris buffer (1 M, pH 8.5) before applying to the sensor array.

We first tested the effectiveness of coupling Ig protein removal with Protein L beads with Ig protein detection by our array sensor using samples mimicking the deficiencies prepared in 1× PBS buffer. The situation mimicking the normal condition contained all three proteins at the molar ratio of IgA:IgM:IgG = 1:1:8, with the concentrations of IgA and IgM being 200 μg/mL, and that of IgG being 1600 μg/mL. The state of IgA deficiency had IgA:IgM:IgG = 0:1:8; IgM deficiency had IgA:IgM:IgG = 1:0:8; and IgG deficiency contained IgA:IgM:IgG = 1:1:0. The proteins were initially spiked to the 1×PBS buffer, then extracted by Protein L beads. After being eluted off the Protein L beads, they were detected by our sensor array, or ELISA. Once the effectiveness of the method was confirmed, we tested detection of Ig deficiency by spiking the corresponding proteins to serum.

Enzyme-Linked Immunosorbent Assay. ELISA was used here to verify the results of sensor array. In a typical experiment, Ig protein samples were first diluted to a proper concentration (< 20 μg/mL) with PBS buffer. For each well, 50 μL diluted solutions was added and incubate at 4°C overnight. The solution was removed, and plate was washed twice with PBS buffer before adding the blocking solution (1% BSA in PBS). After 2 hours incubation, BSA was removed and plate was washed twice with PBS buffer. HRP labelled antibody was added and incubate for another 2 hours at room temperature. The plate was washed 4 times before adding the luminescence agents (Pierce™ ECL Western Blotting Substrate, Thermo Fisher Scientific). The chemiluminescence was collected within 10 minutes by the GloMax-Multi Detection System (Promega) with default settings. Standard curve was prepared the same way with series dilution of IgA, IgG and IgM protein stock.

Supporting Figures

1. Discrimination of Immunoglobulin protein in solution.

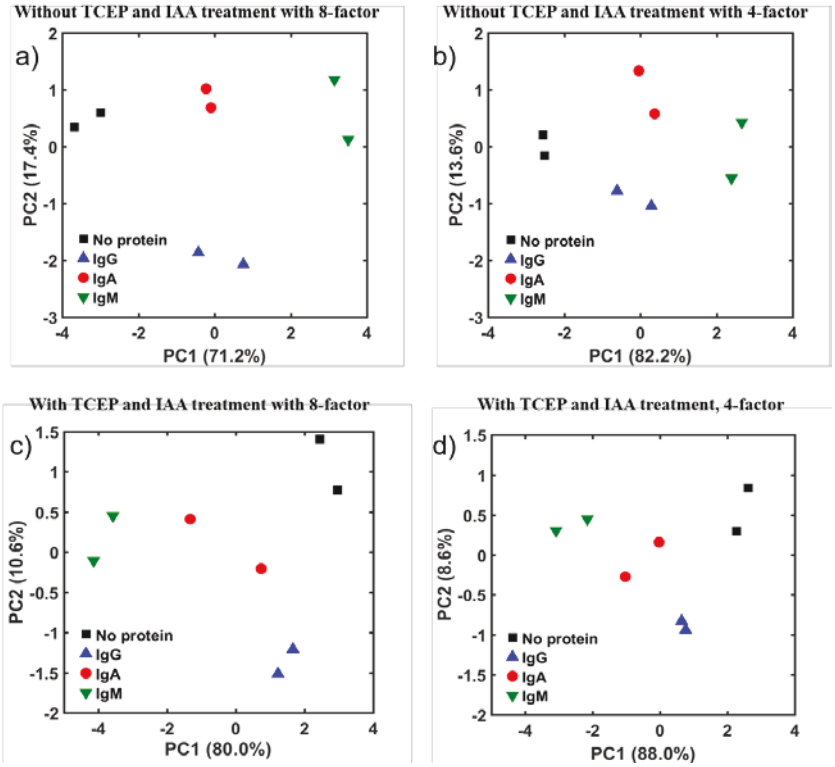

Figure S-1. PCA score plots of data from Figure 2a and 2b with all 8 factors: **1**·**4**, **2**·**4** or **3**·**4** at pH 7.4 or 9.0 and **1**·**5** at pH 7.4 with [**5**] = 1.5 or 40 μM (a, c) or 4 factors: **1**·**4**, **2**·**4** or **3**·**4** at pH 7.4 and **1**·**5** at pH 7.4 with [**5**] = 40 μM (b, d).

2. Protein and cavitand binding mechanism study

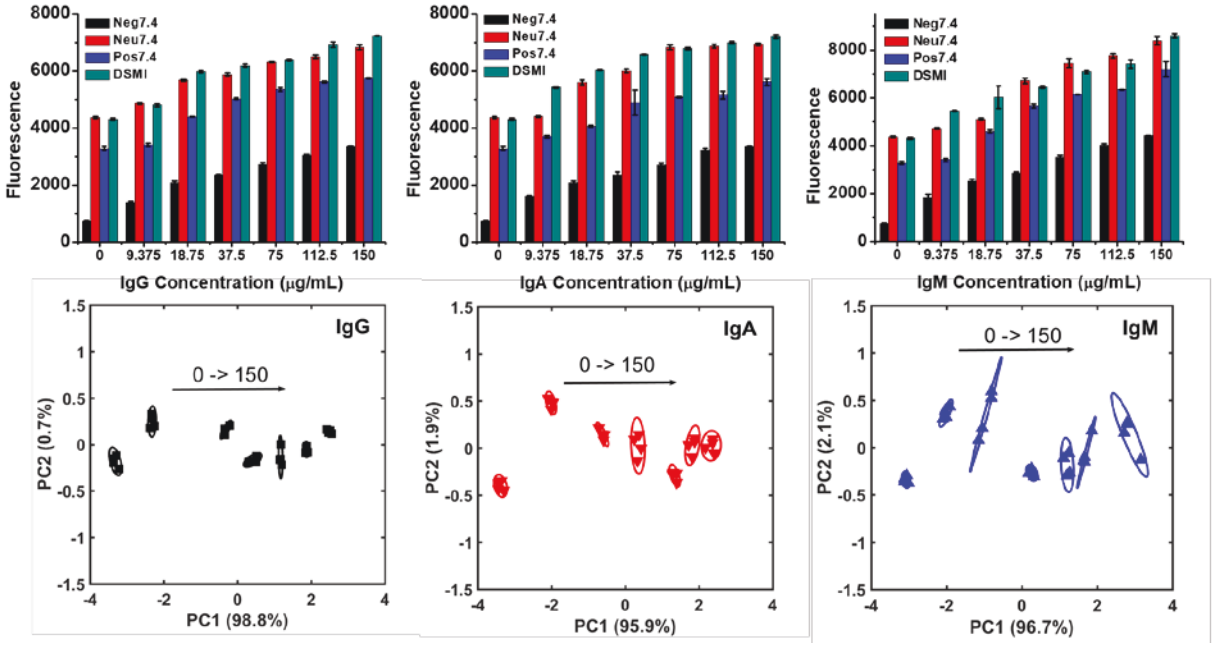

Figure S-2. Raw fluorescence response and PCA plot of IgG, IgA and IgM with 4 factors sensor array. Concentration of proteins are from low to high: 0, 9.375, 18.75, 37.5, 75, 112.5 and 150 μg/mL.

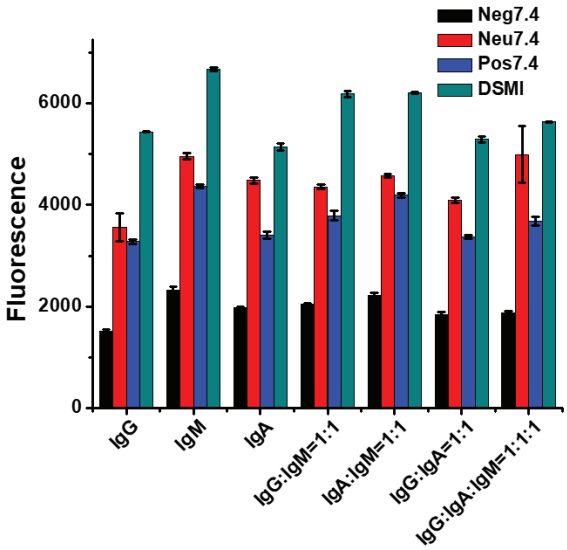

Figure S-3. Raw fluorescence response for protein mixture detection. The total amount of Ig protein in each assay is 150 μg/mL.

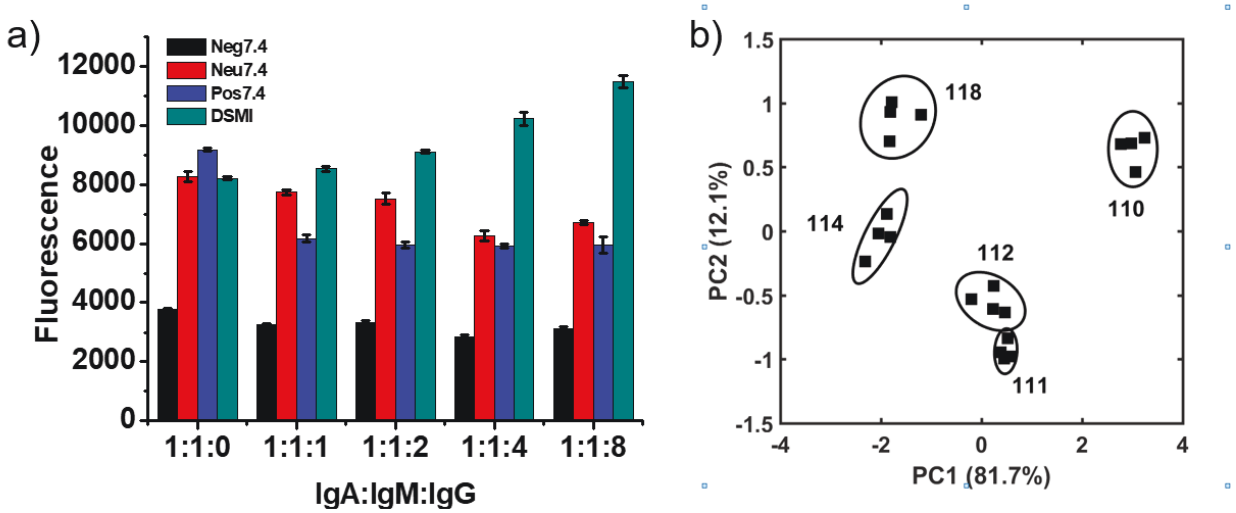

Figure S-4. Detection of IgG in presence of IgA and IgM in 10 mM PBS. IgA = 50 μg/mL; IgM = 50 μg/mL; IgG = 0 – 400 μg/mL.

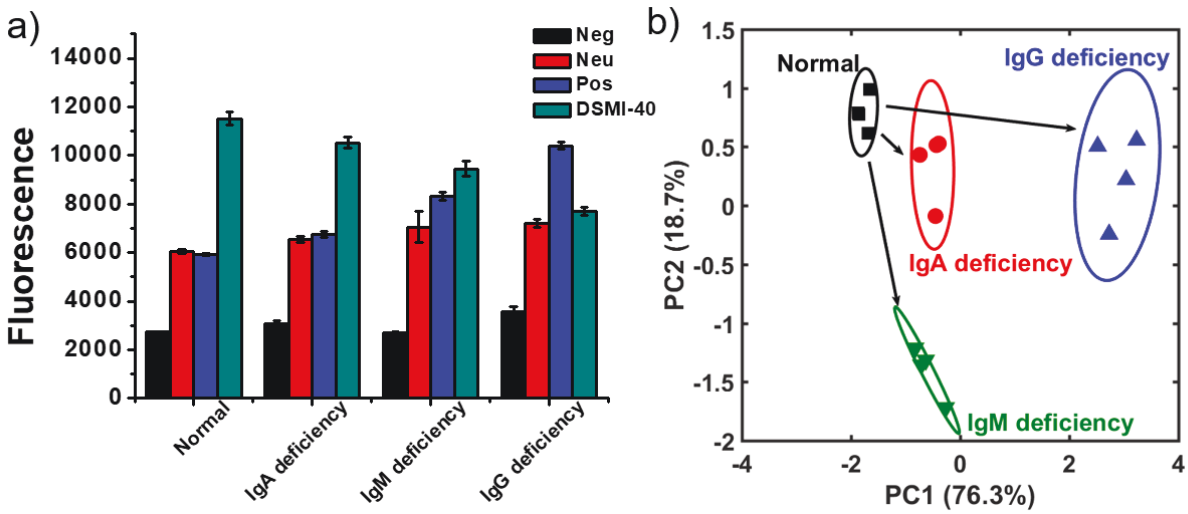

Figure S-5. Mimic of Immunoglobulin deficiencies in 1×PBS buffer. Normal stands for IgA:IgM:IgG = 1:1:8; IgA deficiency stands for IgA:IgM:IgG = 0:1:8; IgM deficiency stands for IgA:IgM:IgG = 1:0:8; IgG deficiency stands for IgA:IgM:IgG = 1:1:0. IgA = 200 μg/mL, IgM = 200 μg/mL and IgG = 1600 μg/mL.

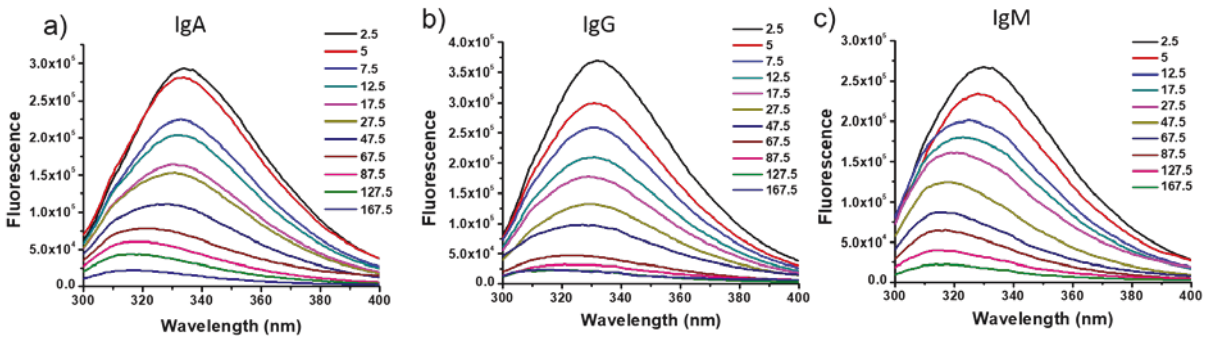

Figure S-6. Cavitand quenching effect of native tryptophan fluorescence of IgA (a), IgG (b) and IgM (c). Excitation = 280 nm. Cavitand concentration increasing from 2.5 µM to 167.5 µM. [protein] = 400 µg/mL

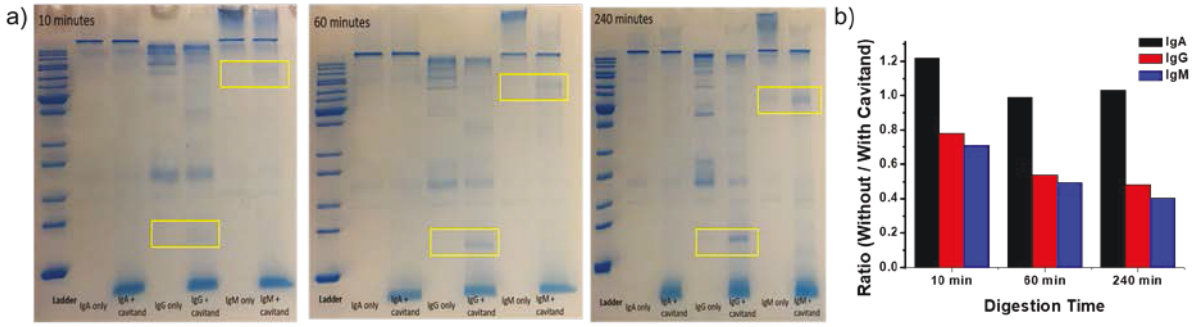

Figure S-7. (a) Trypsin digestion of Immunoglobulin protein with and without cavitand. Protein: cavitand = 1:1 mass ratio. Trypsin: Protein = 1: 50 mass ratios. [Protein] = 200 µg/mL. (b) The bar plot compares the intensity of the product band enclosed in the yellow rectangle.

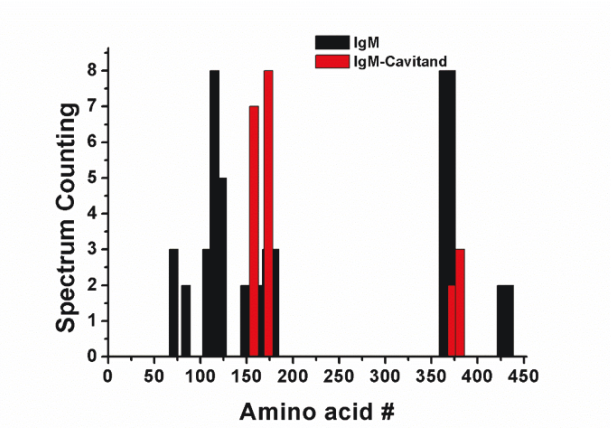

Amino acid #
1-453

Sequence length	453
Hydrophobicity	80.85
GRAVY	-0.32
MW average	49440.2953 g/mol
MW monoisotopic	49408.5824
Theoretical pI	6.3

Amino acids
Hydrophobic: 39.74%
Acidic: 9.71%
Basic: 11.04%
Neutral: 39.51%

Amino Acid
#75-125

Sequence length	50
Hydrophobicity	43.59
GRAVY	-0.37
MW average	5495.4213 g/mol
MW monoisotopic	5491.8540
Theoretical pI	7.3

Amino acids
Hydrophobic: 48%
Acidic: 12%
Basic: 16%
Neutral: 24%

Amino Acid
#350-400

Sequence length	50
Hydrophobicity	55.52
GRAVY	-0.06
MW average	5536.4513 g/mol
MW monoisotopic	5532.7464
Theoretical pI	7.2

Amino acids
Hydrophobic: 52%
Acidic: 6%
Basic: 8%
Neutral: 34%

Amino Acid #
150-200

Sequence length	50
Hydrophobicity	38.80
GRAVY	-0.60
MW average	5396.0093 g/mol
MW monoisotopic	5392.6081
Theoretical pI	4.5

Amino acids
Hydrophobic: 28%
Acidic: 14%
Basic: 10%
Neutral: 48%

Figure S-8. LC-MS/MS counts of peptides obtained after limited digestion with trypsin. 20 µg/mL protein and cavitand **1** were used.

3. Protein quantification with sensor array

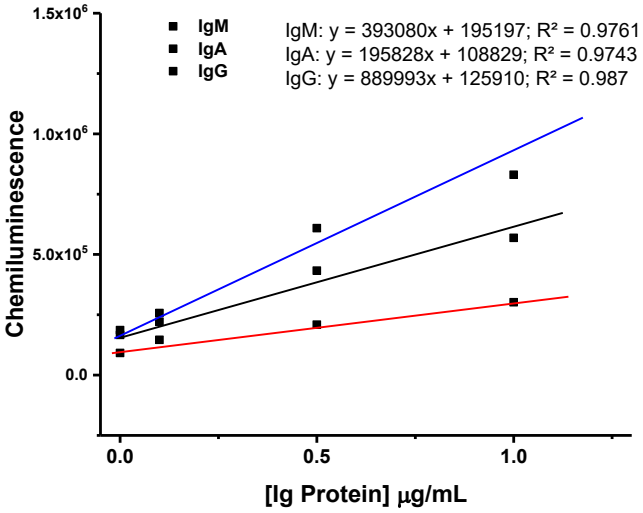

Figure S-9. ELISA calibration curves used for quantification of Ig proteins extracted from serum.

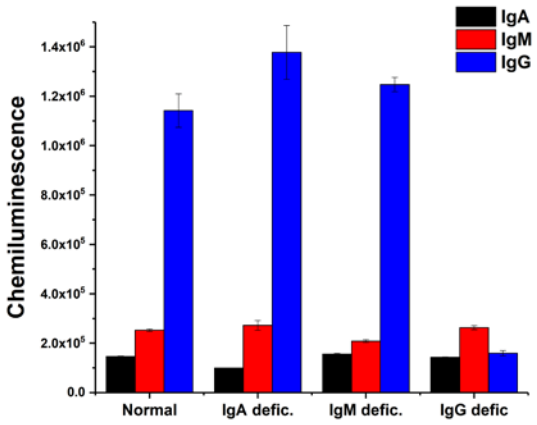

Figure S-10. Chemiluminescence obtained from ELISA for detection of Ig proteins extracted from serum. The protein samples were diluted 400 times before measurement.

Supporting Tables

Table S-1. Fc Region of Five immunoglobulin isotypes. Protein sequences of Fc region were obtained from UniProt. The MW, PI, GRAVY score and Aliphatic Index were calculated using ProtParam tool with default settings.

Protein Fc Region	IgG	IgA	IgM	IgD	IgE
NO. of amino acids	340	346.5	453	384	428
MW	37308	37122	49439	42353	47019
pI	7.8825	5.97	6.35	8.38	8.39
GRAVY	-0.445	-0.237	-0.319	-0.566	-0.375
Aliphatic Index	67.04	72.16	71.39	67.32	67.41

Table S-2. PCA Loading scores for each factor in the 8 factor cavitand guest system.

Factors	**Component 1**	**Component 2**
Neg7.4	-0.376	-0.25
Neg9	-0.382	
Neu7.4	-0.376	-0.179
Neu9	-0.36	0.153
Pos7.4	-0.323	-0.545
Pos9	-0.36	
1.5 μM DSMI	-0.272	0.714
40 μM DSMI	-0.366	0.272

Table S-3. Jackknife analysis of the fluorescence data shown in Figure 2a.

	IgA	**IgD**	**IgE**	**IgG**	**IgM**	**Correctness**
IgA	**4**	**0**	**0**	**0**	**0**	**100%**
IgD	**0**	**4**	**0**	**0**	**0**	**100%**
IgE	**0**	**0**	**4**	**0**	**0**	**100%**
IgG	**0**	**0**	**0**	**4**	**0**	**100%**
IgM	**0**	**0**	**0**	**0**	**4**	**100%**
Total	**4**	**4**	**4**	**4**	**4**	**100%**

Table S-4. Adsorption ratio of protein L beads to each of the three Immunoglobulin protein. 0.125mg beads were used here.

IgG (Total) μg	IgG (adsorbed) μg	Ratio
3.38	1.64	48.73%
6.75	4.23	62.63%
13.50	8.96	66.38%
20.25	13.60	67.15%
31.50	19.40	61.58%
40.50	23.77	58.69%

IgA (Total) μg	IgA (adsorbed) μg	Ratio
3.08	1.02	33.15%
6.16	2.93	47.52%
12.32	6.26	50.79%
18.48	8.09	43.77%
28.75	11.49	39.98%
36.97	13.18	35.64%

IgM (Total) μg	IgM (adsorbed) μg	Ratio
4.67	1.52	32.64%
9.33	3.53	37.81%
20.99	12.38	58.96%
27.99	15.97	57.05%
43.54	23.88	54.84%
55.98	34.83	62.22%

Table S-5. Elution efficiency of IgA, IgG and IgM with protein L beads.

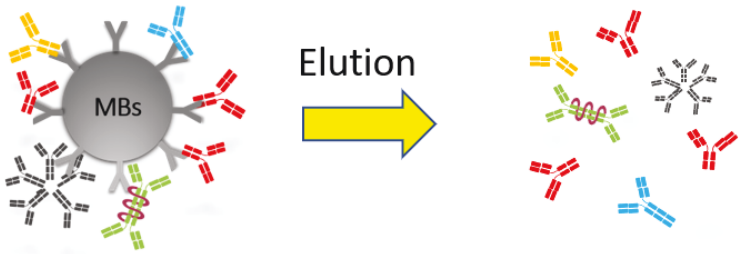

	Total Protein (μg)	Adsorbed (μg)	Eluted (μg)	Elution efficiency
IgA	104.67	63.32	60.98	96.31%
IgG	108.83	71.64	58.66	81.89%
IgM	113.64	59.19	55.69	94.09%

4. References

1. S. M. Biros, E. C. Ullrich, F. Hof, L. Trembleau and J. Rebek, Jr. *J. Am. Chem. Soc.* 2004, **126**, 2870-2876.
2. A. R. Far, A. Shivanyuk and J. Rebek, Jr. *J. Am. Chem. Soc.* 2002, **124**, 2854-2855.
3. Y. Liu, L. Perez, M. Mettry, A. D. Gill, S. R. Byers, C. J. Easley, C. J. Bardeen, W. Zhong and R. J. Hooley, *Chem. Sci.* 2017, **8**, 3960-3970.